Featured in Physics

Persistent Currents in Rings of Ultracold Fermionic Atoms

Yanping Cai, Daniel G. Allman, Parth Sabharwal, and Kevin C. Wright*

Department of Physics and Astronomy, Dartmouth College, 6127 Wilder Laboratory, Hanover, New Hampshire 03755, USA

(Received 5 April 2021; revised 31 December 2021; accepted 1 March 2022; published 12 April 2022)

We have produced persistent currents of ultracold fermionic atoms trapped in a ring, with lifetimes greater than 10 sec in the strongly interacting regime. These currents remain stable well into the BCS regime at sufficiently low temperature. We drive a circulating BCS superfluid into the normal phase and back by changing the interaction strength and find that the probability for quantized superflow to reappear is remarkably insensitive to the time spent in the normal phase and the minimum interaction strength. After ruling out spontaneous current formation for our experimental conditions, we argue that the reappearance of superflow is due to weak damping of normal currents in this limit. These results establish that ultracold fermionic atoms with tunable interactions can be used to create matter-wave circuits similar to those previously created with weakly interacting bosonic atoms.

DOI: 10.1103/PhysRevLett.128.150401

Progress in understanding quantum fluids has often been made by considering spherical, cylindrical, toroidal, or more exotic geometries [1], and circuits built from quantum materials have many important applications including quantum computing. Quantum gases with periodic boundary conditions provide unique opportunities for exploring quantum many-body physics, especially where it is possible to bias a circuit with an external flux [2,3]. One crucial characteristic of such circuits is that they can support quantized currents that flow without being driven by an external power source. Persistent nonequilibrium currents are commonly understood to occur in superconducting [4] and superfluid [5] phases, but equilibrium persistent currents can also appear in normal conducting phases around closed paths shorter than the coherence length [6–8]. The current response of such circuits to external flux often conveys important information about the state of the system [9].

Previous experiments with multiply connected ultracold gases have utilized weakly interacting atomic Bose-Einstein condensates (BEC) in magnetic and optical traps [10–17]. Experiments on ring BECs have demonstrated the existence of metastable currents [11,13] and quantized phase slips [18,19]. Bosonic superfluid circuits have been constructed by incorporating Josephson junctions [20–22], and the experimental usefulness of multiply connected quantum gases has been demonstrated by studies of collective-mode precession [23], spontaneous currents [24–26], quantum turbulence [14], propagation of shock waves [27], the stability of supersonic superfluid flows [28,29], and more [30].

Fermionic quantum gases provide access to a rich variety of physics distinctly different from that of purely bosonic systems. Furthermore, magnetic fields can often be used to continuously tune interactions between fermionic atoms from the weakly attractive limit where BCS pairing can occur to the weakly repulsive limit where the atoms can form a BEC of weakly bound molecules. Fermionic superfluidity has been extensively studied throughout this BEC-BCS crossover, including experimental observations of an interaction-dependent critical velocity in three dimensions [31], and very recently in two dimensions [32]. Josephson junctions and quantum point contacts have also been realized in singly connected fermionic quantum gases [33,34].

In this Letter we report the first creation of a multiply-connected superfluid "circuit" in an ultracold Fermi gas, and show that it is possible to reliably create and detect quantized currents in this system. We demonstrate that currents can survive well into the fragile BCS regime and examine the decay and revival of currents after quenches to the normal phase in this limit, establishing a foundation for other proposed experiments involving quantum gases in rings and ring lattices [2,3,35–41].

In these experiments, we use a quantum degenerate gas of ^{6}Li atoms in an equal mixture of the lowest-energy spin states ($|m_J = -1/2, m_I = 1\rangle$ and $|m_J = -1/2, m_I = 0\rangle$). Interactions between atoms in these two states are attractive (repulsive) at magnetic fields above (below) a broad (> 10 mT) Feshbach resonance at 83.2 mT. To create a persistent current, we must have a continuous (pair) superfluid around a closed path, which requires a trap with a smooth ring-shaped potential minimum and cooling the system below a critical temperature which depends on the interaction strength and density. We created an optical ring trap with two red-detuned laser beams, a horizontal "sheet" beam ($\lambda = 1068$ nm, horizontal waist 290 μm, vertical waist 7 μm) and a vertical ring-pattern beam [$\lambda = 780$ nm, average radius 12.0(1) μm, radial $1/e^2$ half-width 2.2(1) μm] (see Supplemental Material [42]).

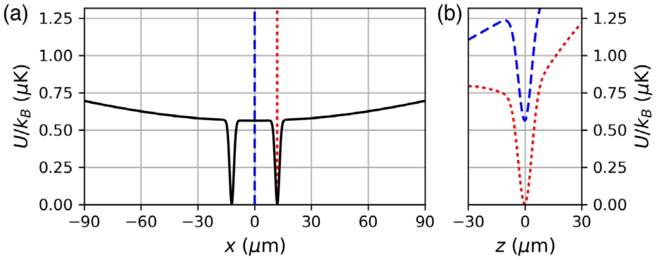

FIG. 1. Cross sections of an idealized model of the potential experienced by a ^{6}Li atom in our "ring-dimple" optical trap in its final configuration (the potential is twice as deep for molecules). (a) Black line is the potential along a horizontal line through the center of symmetry, transverse to the direction of propagation of the sheet beam. The radial trap frequency for atoms away from the ring minimum is 37(5) s^{-1}. (b) Vertical cross section of the trap potential at $r = 0$ (dashed line, blue online) and $r = 12.0$ μm (dotted line, red online), as indicated by corresponding vertical lines in (a). The vertical trap frequency is $1.5(1) \times 10^3$ s^{-1} for atoms near the ring potential minimum, and $1.4(1) \times 10^3$ s^{-1} away from the ring beam. The plot vertical range is from $U_{\mathrm{trap}} = 0$ at the ring minimum to the "trap-off" potential in the midplane of the ring (1.32 μK).

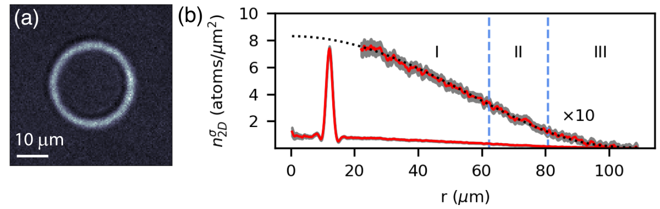

FIG. 2. (a) Absorption image (10 averaged) of an equal spin mixture of ^{6}Li atoms in the trap potential of Fig. 1, with 1×10^4 atoms in each spin state. A magnetic field of 107.4 mT has been used to tune the scattering length to -179 nm. The density peak is at $r = 12.0(2)$ μm. This is a 50×50 μm region cropped from a 215×215 μm image. (b) Radial column density obtained by azimuthal averaging over the full field of view. The plot is shown vertically rescaled $\times 10$ for $r > 20$ μm to emphasize the broad halo extending to $r = 100$ μm. The black dotted line is the expected density profile ($\times 10$) for an ideal Fermi gas in our trap at $T = 25$ nK. In region I the system is 3D degenerate, II is quasi-2D degenerate, and III is quasi-2D thermal. Gray band: 2σ variation of $n_{2\mathrm{D}}(r)$ when calculated separately for each image in the set.

The next critical requirement is to achieve and maintain low enough temperatures to study supercurrents over a wide range of interaction strengths. We loaded the atoms into the ring trap with the sheet beam initially at high power (4 W), and performed final evaporative cooling with the magnetic field near resonance (82.0 mT) by decreasing the sheet beam power to 40 mW while holding the ring beam power at 0.85 mW. Evaporation occurred as molecules fell out of the bottom of the ring region where the potential barrier was lowest; the gravitational gradient reduced the final evaporation depth to an estimated $k_B 0.80(5)$ μK as shown in Fig. 1(b).

After evaporation there were $1.0(1) \times 10^4$ atoms in each spin state, paired into weakly bound molecules with strong repulsive interactions. The chemical potential (μ) was high enough that most of the molecules were not localized to the ring and formed a wide, thin disk in the radially weak, vertically strong harmonic potential of the sheet beam [$\nu_r = 37(5)$ s^{-1}, $\nu_z = 1.4(1) \times 10^3$ s^{-1}]. The fraction of the population in this "halo" increased if we subsequently tuned interactions to the weakly attractive (BCS) limit where $\mu \approx E_F$ (Fermi energy). From a model of our trap we calculated that in this limit $E_F = h16(1) \times 10^3$ $\mathrm{s}^{-1} = k_B 0.77(6)$ μK (see Supplemental Material [42]). The radial trap frequency for atoms (and molecules) near the ring potential minimum was $\nu_r = 4.0(2) \times 10^3$ s^{-1}.

The low-density halo was hardly visible in absorption images, but easily observed in radial plots of the column density after azimuthal averaging. Figure 2 shows averaged results from 10 runs where the field was ramped from 82.0 to 107.4 mT before imaging the atoms in the ring. Figure 2(a) has been cropped to show ring density variations (10% peak to peak) in more detail. Figure 2(b) shows the column density, $n_{2\mathrm{D}}(r)$, obtained from the full-frame image by averaging data in radial bins 1 μm wide. Fitting the density profile for $r > 20$ μm with a model of an ideal Fermi gas in our trap potential indicated that $T = 25(5)$ nK. Because $T < h\nu_z/k_B = 72$ nK, we accounted for the crossover from 3D to quasi-2D in the outer regions of the halo (see Supplemental Material [42]). The best fit of this model to the data for $r > 20$ μm is shown in Fig. 2(b) as a dotted black line.

When we ramped from 82.0 to 68.0 mT (BEC regime) we found that $n_{2\mathrm{D}}$ for $r > 20$ μm had the Gaussian profile expected for a thermal gas of molecules at 90(3) nK. Temperature changes are expected for isentropic interaction ramps because the temperature dependence of the entropy is different in the BEC and BCS limits [43]. The minimum temperature we observed in the BCS regime was likely limited by heating due to hole creation by collisions with background gas molecules [44]. Fermionic systems are especially sensitive to heating at low temperatures. Retaining a large part of the population in a low-density halo increases the average heat capacity per particle and reduces the heating rate, which was important for the experiments described below.

Our general procedure for creating persistent currents and studying their stability in the BCS regime was the following: We prepared a strongly interacting molecular BEC at $B = 82.0$ mT as described above, then initialized the current state by stirring with a blue-detuned laser beam that created a localized repulsive potential. We then changed the interaction strength adiabatically by ramping the magnetic field up to the BCS regime, then ramped back to 82.0 mT. Finally, we ramped to the BEC regime and used

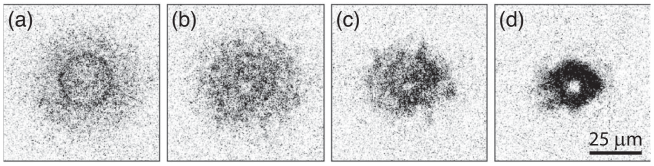

FIG. 3. Evolution of a molecular BEC during the last part of the procedure for measuring the current state of the ring. (a) Absorption image showing the vertical column density after relaxing the ring confinement and sweeping the magnetic field from 82.0 to 68.3 mT to lower the interaction energy. (b)–(d) Evolution of the density profile after the optical trap is shut off, for 1.5, 3.5, and 5.5 ms time of flight. Radial magnetic lensing improves the signal-to-noise ratio in detecting the vortex core associated with the persistent current. Each image is from a separate realization of the experiment.

a self-interference technique to determine the final current state of the ring.

It was challenging to adapt the supercurrent detection procedures developed with ring BECs [19,22,23,45–47] to rings of strongly interacting light fermionic atoms. Lower condensate fraction in fermionic systems, rapid expansion due to the high chemical potential, and pair breaking in the BCS limit all reduce coherence and the signal to noise ratio in images. These procedures were most effective in the BEC limit after lowering the interaction energy as much as possible. While the field was still at 82.0 mT, we relaxed the radial confinement by lowering the ring beam power to 5% of its initial value over 100 ms, changing the profile of the cloud to that of Fig. 3(a). This transformed a current with winding number ℓ into ℓ singly charged vortices in the central region that were too small to detect optically. We then swept the magnetic field from 82.0 to 68.3 mT in 20 ms, reducing the scattering length by 96%. (Ramping to even lower field caused the three-body loss rate to become too high during the detection procedure.) Next, we turned off the trap and allowed the atoms to evolve for 5.5 ms in a magnetic field with a weak radial curvature. This caused radial focusing, which increased the signal-to-noise ratio in the absorption image taken at the end, using the $|m_J = -1/2, m_I = 1\rangle \rightarrow |m_J = -3/2, m_I = 1\rangle$ transition. Figure 3 shows typical evolution of the density profile for a system prepared in an $|\ell| = 1$ current state. The single hole indicates the presence of a single vortex [48].

In this Letter we initialized the current state by stirring [18,49], but note that phase imprinting is also possible [11,19,50,51] and was demonstrated with fermions by another group recently [52]. In our system spontaneous currents often appeared during initial formation of the molecular BEC, and stirring allowed deterministic preparation of a selected current state even when the initial current state was uncertain, which is not possible with phase imprinting. We created a repulsive stirring potential with a steerable blue-detuned beam [$\lambda = 635$ nm, radius $6(1)$ μm]. To initialize the system in a zero-current state, we kept the beam stationary at one point on the ring, increased the laser power linearly over 100 ms until the peak of the repulsive potential was around 1.5 μ, held for 100 ms, then ramped the beam off in 100 ms. After this procedure the probability of detecting a nonzero current was $0.00^{+0.02}_{-0.00}$ (uncertainties are 1σ Bayesian binomial confidence intervals [53]).

To create a current we accelerated the stirring beam around the ring at 100 rad/s^2 up to a maximum angular velocity that we held constant for 300 ms, then ramped the beam power off linearly in the final 100 ms. The angular frequency of a quantized current of pairs with winding number ℓ in our ring was $\ell\Omega_0 \equiv \ell\hbar/(m_{\mathrm{pair}}R^2) = 2\pi\ell 5.83(2)$ rad $\cdot$ s^{-1}. The probability of creating an $\ell = 1$ current ($P_{\ell=1}$) became significant for stirring frequencies near 0.5 Ω_0, increasing to ≈ 1 above 0.7 Ω_0. We have created higher current states by stirring at higher angular velocities, but focus here on creation and decay of the $\ell = 1$ state.

In our system $T/T_c < 0.5$ over a significant range of interaction strengths near resonance, and under these conditions persistent currents survived for up to 10 sec, limited by losses from background gas collisions ($1/e$ lifetime 12 sec) or three-body collisions. (When losses reduced the total atom number below 10^4 we could no longer distinguish vortices from thermal density fluctuations using the detection procedure described above.) When ramping into the BCS regime T_c falls exponentially, and thermally activated phase slips to lower energy states should occur as $T/T_c \rightarrow 1$ at the weakest point of the ring [54–56]. We estimated the local Fermi temperature at that point to be $T'_F = 0.69(1)$ μK and the inverse Fermi wave number was $1/k'_F = 0.24(1)$ μm. Neglecting small corrections due to trap confinement [57], the expected critical temperature for the superfluid transition is $T_c \approx 0.277 T_F e^{-\pi/2k_F|a|}$ [58]. Given our measurement that $T = 25(5)$ nK in the BCS limit, the superfluid density should vanish at the weak point of the ring when $B = 106(3)$ mT $[-1/k'_F a = 1.3(1)]$.

To characterize the decay of the current around this interaction strength, we prepared the system in the $\ell = 1$ current state at $B_i = 82.0$ mT, swept the magnetic field in 100 ms to a value B_{max} in the BCS regime, then swept back to B_i in 100 ms before measuring the final current state. This sweep rate is slow enough to be adiabatic, causing no detectable excitation of collective modes. We found that the current did not decay for $B_{\mathrm{max}} < 98.0$ mT $(-1/k'_F a < 1)$. The data in Fig. 4 show the decreasing probability of detecting an $\ell = 1$ current ($P_{\ell=1}$) for B_{max} from 98.0 up to 107.8 mT (our technical limit). The decrease of $P_{\ell=1}$ over the range from 98.0 to 105 mT is consistent with expectations that the rate of decay via thermally activated phase slips increases as $T/T_c \rightarrow 1$ [54–56,59]. In the $l = 1$ current state, the kinetic energy of the pairs is small enough $(mv^2/k_B T < 0.01)$ that its contribution to pair-breaking

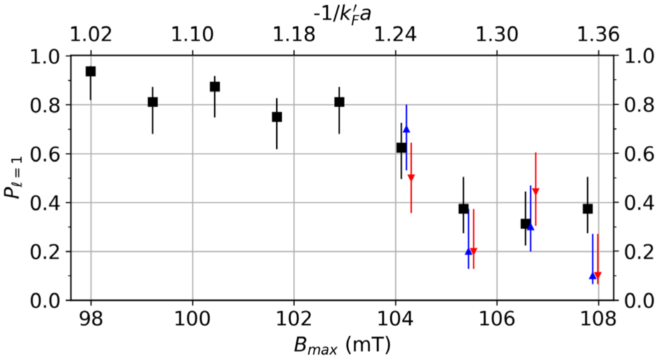

FIG. 4. Probability of detecting an $\ell = 1$ current after preparing the superfluid ring in that state near resonance (82 mT) then ramping the interactions into the BCS regime and back. The horizontal axis is the maximum magnetic field ($B_{\max}$) used in the ramp (lower scale) and the interaction parameter $-1/k_F'a$ (upper scale) where a is the scattering length and $2\pi/k_F' = 1.49$ μm is the local Fermi wavelength at the "weak point" of the ring. Black squares represent 16 runs averaged, where B was ramped up and down in 0.2 ms with no hold time at $B_{\max}$. Triangles are data (10 runs each point) obtained when holding at $B_{\max}$ for 0.1 s (upright, blue online) and 0.2 s (inverted, red online), and are horizontally offset (from squares) for clarity. Uncertainties are 1σ Bayesian binomial confidence intervals [53].

and current decay via phase slips should be negligible as $T/T_c \to 1$.

Because our detection procedure requires ramping back to the BEC limit, interpretation of the data when any part of the ring is quenched to the normal phase requires consideration of spontaneous current formation, the damping of the normal current, and the effect of thermal phase fluctuations. Spontaneous currents can appear during sufficiently rapid merging of independent superfluid regions [24,60]. This can occur if there is significant azimuthal variation in the ring potential minimum [26], or via the Kibble-Zurek mechanism during a fast quench to the superfluid phase [25,61]. To determine whether spontaneous current formation was significant for our experimental conditions we prepared the atoms in the $\ell = 0$ state and measured the final current state after similar ramps to the BCS regime. The probability of observing $\ell \neq 0$ was $0.04^{+0.08}_{-0.01}$, indicating that the nonzero probabilities in Fig. 4 can be attributed to initializing the system in the $\ell = 1$ current state.

When a normal fluid circulating around a ring is driven into a superfluid phase, it will most likely form in the quantized current state that minimizes the free energy [62,63]. When phase fluctuations are small the distribution of final current states is sharply peaked, with the probability of one state near unity. Large phase fluctuations broaden the distribution and make the result nondeterministic. When $B_{\max}$ is high enough that the ring is broken by a region in the normal phase, damping of the current (and excitations in the remaining superfluid) should cause $P_{\ell=1}$ to fall to zero eventually. For linear ramps up to $B_{\max}$ and immediately back down, $P_{\ell=1}$ did not fall to zero and was nearly the same for the highest three values of $B_{\max}$, with an average value of $0.35^{+0.07}_{-0.06}$ (see Fig. 4).

To obtain more information about the timescale for damping we repeated the procedure, adding a hold time of either 0.1 or 0.2 s at the highest values of $B_{\max}$ (see offset data in Fig. 4). Again, $P_{\ell=1}$ did not fall to zero, and the dependence on $B_{\max}$ was weak (0.04 ± 0.1 /mT for the three highest values of $B_{\max}$, similar for 0.1 and 0.2 s hold). For a 0.1 s hold, the average value of $P_{\ell=1}$ for the three highest values of $B_{\max}$ was $P_{\ell=1} = 0.20^{+0.09}_{-0.05}$. For 0.2 s it was $0.24^{+0.09}_{-0.06}$. Fitting to these average values for each hold time, the estimated decay time was 0.5 s, with a 1σ lower bound of 0.25 s. This is longer than our ramp times, and much longer than the few-millisecond timescale for sound to propagate around the ring. We did not systematically investigate longer hold times because heating was non-negligible and we could no longer treat the temperature as nearly constant. The most plausible explanation for the data at the right of Fig. 4 is that the average total current remained significantly greater than zero even when part of the ring was driven normal, and thermal phase fluctuations and/or long-wavelength excitations in the superfluid broadened the distribution of final current states after the superfluid ring reconnected. It should be possible to study these current decay and reconnection dynamics in detail in future experiments using interferometric techniques in a "target" or double-ring trap configuration [22].

In conclusion, we have studied persistent currents in a fermionic matter-wave circuit across a range of interaction strengths. We initialized the system in a selected current state and detected single-quantum changes in the current state. We maintained low enough temperatures for supercurrents to survive well into the BCS regime and found that the potential was smooth enough for normal currents to be relatively long-lived. These results also provide a framework enabling future studies of transport and nonequilibrium phenomena in rings of ultracold fermionic atoms. We observed spontaneous currents for faster interaction ramps, indicating an opportunity to study the Kibble-Zurek mechanism with fermions [64] in the annular geometry originally proposed by Zurek [65]. In a spin-imbalanced ring of fermionic atoms it may be possible to create π-Josephson junctions [66] and search for evidence of unconventional spin-polarized superfluid phases [36,67]. Finally, the tight transverse confinement achieved in these experiments could be increased to realize quasi-2D and 1D rings of fermions with tunable interactions, where non-Fermi-liquid behavior is expected and parity effects can be significant [3].

We thank J. Evans, S. Khatry, L. Bezerra, and A. Woronecki for key technical contributions to the experimental apparatus and recognize D. Adams, C. Grant, and

D. Collins for critical engineering support. We also thank R. Onofrio for insightful discussions about ultracold fermionic systems. This work was supported by the NSF (Grant No. PHY-1707557).

*Kevin.Wright@Dartmouth.edu

[1] E. Fradkin, *Field Theories of Condensed Matter Physics* (Cambridge University Press, Cambridge, England, 2013).
[2] L. Amico, A. Osterloh, and F. Cataliotti, Quantum Many Particle Systems in Ring-Shaped Optical Lattices, Phys. Rev. Lett. **95**, 063201 (2005).
[3] G. Pecci, P. Naldesi, L. Amico, and A. Minguzzi, Probing the BCS-BEC crossover with persistent currents, Phys. Rev. Research **3**, L032064 (2021).
[4] B. S. Deaver and W. M. Fairbank, Experimental Evidence for Quantized Flux in Superconducting Cylinders, Phys. Rev. Lett. **7**, 43 (1961).
[5] P. P. J. Bendt, Superfluid helium critical velocities in a rotating annulus, Phys. Rev. **127**, 1441 (1962).
[6] M. Büttiker, Y. Imry, and R. Landauer, Josephson behavior in small normal one-dimensional rings, Phys. Lett. **96A**, 365 (1983).
[7] H. Bluhm, N. C. Koshnick, J. A. Bert, M. E. Huber, and K. A. Moler, Persistent Currents in Normal Metal Rings, Phys. Rev. Lett. **102**, 136802 (2009).
[8] A. C. Bleszynski-Jayich, W. E. Shanks, B. Peaudecerf, E. Ginossar, F. von Oppen, L. Glazman, and J. G. E. Harris, Persistent currents in normal metal rings, Science **326**, 272 (2009).
[9] W. A. Little and R. D. Parks, Observation of Quantum Periodicity in the Transition Temperature of a Superconducting Cylinder, Phys. Rev. Lett. **9**, 9 (1962).
[10] S. Gupta, K. W. Murch, K. L. Moore, T. P. Purdy, and D. M. Stamper-Kurn, Bose-Einstein Condensation in a Circular Waveguide, Phys. Rev. Lett. **95**, 143201 (2005).
[11] C. Ryu, M. F. Andersen, P. Cladé, V. Natarajan, K. Helmerson, and W. D. Phillips, Observation of Persistent Flow of a Bose-Einstein Condensate in a Toroidal Trap, Phys. Rev. Lett. **99**, 260401 (2007).
[12] G. D. Bruce, J. Mayoh, G. Smirne, L. Torralbo-Campo, and D. Cassettari, A smooth, holographically generated ring trap for the investigation of superfluidity in ultracold atoms, Phys. Scr. **T143**, 014008 (2011).
[13] S. Beattie, S. Moulder, R. J. Fletcher, and Z. Hadzibabic, Persistent Currents in Spinor Condensates, Phys. Rev. Lett. **110**, 025301 (2013).
[14] T. W. Neely, A. S. Bradley, E. C. Samson, S. J. Rooney, E. M. Wright, K. J. H. Law, R. Carretero-González, P. G. Kevrekidis, M. J. Davis, and B. P. Anderson, Characteristics of Two-Dimensional Quantum Turbulence in a Compressible Superfluid, Phys. Rev. Lett. **111**, 235301 (2013).
[15] B. E. Sherlock, M. Gildemeister, E. Owen, E. Nugent, and C. J. Foot, Time-averaged adiabatic ring potential for ultracold atoms, Phys. Rev. A **83**, 043408 (2011).
[16] P. Navez, S. Pandey, H. Mas, K. Poulios, T. Fernholz, and W. von Klitzing, Matter-wave interferometers using TAAP rings, New J. Phys. **18**, 075014 (2016).
[17] M. de Goër de Herve, Y. Guo, C. De Rossi, A. Kumar, T. Badr, R. Dubessy, L. Longchambon, and H. Perrin, A versatile ring trap for quantum gases, J. Phys. B **54**, 125302 (2021).
[18] K. C. Wright, R. B. Blakestad, C. J. Lobb, W. D. Phillips, and G. K. Campbell, Driving Phase Slips in a Superfluid Atom Circuit with a Rotating Weak Link, Phys. Rev. Lett. **110**, 025302 (2013).
[19] A. Ramanathan, K. C. Wright, S. R. Muniz, M. Zelan, W. T. Hill, C. J. Lobb, K. Helmerson, W. D. Phillips, and G. K. Campbell, Superflow in a Toroidal Bose-Einstein Condensate: An Atom Circuit with a Tunable Weak Link, Phys. Rev. Lett. **106**, 130401 (2011).
[20] C. Ryu, P. W. Blackburn, A. A. Blinova, and M. G. Boshier, Experimental Realization of Josephson Junctions for an Atom SQUID, Phys. Rev. Lett. **111**, 205301 (2013).
[21] S. Eckel, J. G. Lee, F. Jendrzejewski, N. Murray, C. W. Clark, C. J. Lobb, W. D. Phillips, M. Edwards, and G. K. Campbell, Hysteresis in a quantized superfluid ‘atomtronic’ circuit, Nature (London) **506**, 200 (2014).
[22] S. Eckel, F. Jendrzejewski, A. Kumar, C. J. Lobb, and G. K. Campbell, Interferometric Measurement of the Current-Phase Relationship of a Superfluid Weak Link, Phys. Rev. X **4**, 031052 (2014).
[23] G. E. Marti, R. Olf, and D. M. Stamper-Kurn, Collective excitation interferometry with a toroidal Bose-Einstein condensate, Phys. Rev. A **91**, 013602 (2015).
[24] C. N. Weiler, T. W. Neely, D. R. Scherer, A. S. Bradley, M. J. Davis, and B. P. Anderson, Spontaneous vortices in the formation of Bose–Einstein condensates, Nature (London) **455**, 948 (2008).
[25] L. Corman, L. Chomaz, T. Bienaimé, R. Desbuquois, C. Weitenberg, S. Nascimbène, J. Dalibard, and J. Beugnon, Quench-Induced Supercurrents in an Annular Bose Gas, Phys. Rev. Lett. **113**, 135302 (2014).
[26] M. Aidelsburger, J. L. Ville, R. Saint-Jalm, S. Nascimbène, J. Dalibard, and J. Beugnon, Relaxation Dynamics in the Merging of N Independent Condensates, Phys. Rev. Lett. **119**, 190403 (2017).
[27] Y.-H. Wang, A. Kumar, F. Jendrzejewski, R. M. Wilson, M. Edwards, S. Eckel, G. K. Campbell, and C. W. Clark, Resonant wavepackets and shock waves in an atomtronic SQUID, New J. Phys. **17**, 125012 (2015).
[28] S. Pandey, H. Mas, G. Drougakis, P. Thekkeppatt, V. Bolpasi, G. Vasilakis, K. Poulios, and W. von Klitzing, Hypersonic Bose–Einstein condensates in accelerator rings, Nature (London) **570**, 205 (2019).
[29] Y. Guo, R. Dubessy, M. d. G. de Herve, A. Kumar, T. Badr, A. Perrin, L. Longchambon, and H. Perrin, Supersonic Rotation of a Superfluid: A Long-Lived Dynamical Ring, Phys. Rev. Lett. **124**, 025301 (2020).
[30] L. Amico *et al.*, Roadmap on Atomtronics: State of the art and perspective, AVS Quantum Sci. **3**, 039201 (2021).
[31] W. Weimer, K. Morgener, V. P. Singh, J. Siegl, K. Hueck, N. Luick, L. Mathey, and H. Moritz, Critical Velocity in the BEC-BCS Crossover, Phys. Rev. Lett. **114**, 095301 (2015).
[32] L. Sobirey, N. Luick, M. Bohlen, H. Biss, H. Moritz, and T. Lompe, Observation of superfluidity in a strongly

correlated two-dimensional Fermi gas, Science **372**, 844 (2021).
[33] G. Valtolina, A. Burchianti, A. Amico, E. Neri, K. Xhani, J. a. Seman, A. Trombettoni, A. Smerzi, M. Zaccanti, M. Inguscio, and G. Roati, Josephson effect in fermionic superfluids across the BEC-BCS crossover, Science **350**, 1505 (2015).
[34] D. Husmann, S. Uchino, S. Krinner, M. Lebrat, T. Giamarchi, T. Esslinger, and J.-P. Brantut, Connecting strongly correlated superfluids by a quantum point contact, Science **350**, 1498 (2015).
[35] M. D. Girardeau and E. M. Wright, Rotating Ground States of a One-Dimensional Spin-Polarized Gas of Fermionic Atoms with Attractive inline p-Wave Interactions on a Mesoscopic Ring, Phys. Rev. Lett. **100**, 200403 (2008).
[36] Y. Yanase, Angular Fulde-Ferrell-Larkin-Ovchinnikov state in cold fermion gases in a toroidal trap, Phys. Rev. B **80**, 220510(R) (2009).
[37] M. Roncaglia, M. Rizzi, and J. Dalibard, From rotating atomic rings to quantum Hall states, Sci. Rep. **1**, 43 (2011).
[38] M. J. Edmonds, M. Valiente, G. Juzeliunas, L. Santos, and P. Öhberg, Simulating an Interacting Gauge Theory with Ultracold Bose Gases, Phys. Rev. Lett. **110**, 085301 (2013).
[39] D. Aghamalyan, M. Cominotti, M. Rizzi, D. Rossini, F. Hekking, A. Minguzzi, L. C. Kwek, and L. Amico, Coherent superposition of current flows in an atomtronic quantum interference device, New J. Phys. **17**, 045023 (2015).
[40] S. Ragole and J. M. Taylor, Interacting Atomic Interferometry for Rotation Sensing Approaching the Heisenberg Limit, Phys. Rev. Lett. **117**, 203002 (2016).
[41] M. Metcalf, C.-Y. Lai, K. Wright, and C.-C. Chien, Protocols for dynamically probing topological edge states and dimerization with fermionic atoms in optical potentials, Europhys. Lett. **118**, 56004 (2017).
[42] See Supplemental Material at http://link.aps.org/supplemental/10.1103/PhysRevLett.128.150401 for more detailed information technical information about preparation of the degenerate Fermi gas of Li-6 atoms in the optical ring trap and additional details about the configuration of the trapping beams. It also includes more information about modeling and fits used to obtain estimates of the Fermi energy, temperature, and 3D number density.
[43] L. D. Carr, G. V. Shlyapnikov, and Y. Castin, Achieving a BCS Transition in an Atomic Fermi Gas, Phys. Rev. Lett. **92**, 150404 (2004).
[44] E. Timmermans, Degenerate Fermion Gas Heating by Hole Creation, Phys. Rev. Lett. **87**, 240403 (2001).
[45] N. Murray, M. Krygier, M. Edwards, K. C. Wright, G. K. Campbell, and C. W. Clark, Probing the circulation of ring-shaped Bose-Einstein condensates, Phys. Rev. A **88**, 053615 (2013).
[46] T. Haug, J. Tan, M. Theng, R. Dumke, L.-C. Kwek, and L. Amico, Readout of the atomtronic quantum interference device, Phys. Rev. A **97**, 013633 (2018).
[47] S. Safaei, L.-C. Kwek, R. Dumke, and L. Amico, Monitoring currents in cold-atom circuis, Phys. Rev. A **100**, 013621 (2019).
[48] For $|\ell| > 1$ the multiply charged current fragments into singly charged vortices before the cloud is released, with an $|\ell| = 2$ current resulting in two distinct holes.
[49] J. Brand and W. P. Reinhardt, Generating ring currents, solitons and svortices by stirring a Bose-Einstein condensate in a toroidal trap, J. Phys. B **34**, L113 (2001).
[50] K. C. Wright, L. S. Leslie, A. Hansen, and N. P. Bigelow, Sculpting the Vortex State of a Spinor BEC, Phys. Rev. Lett. **102**, 030405 (2009).
[51] A. Kumar, R. Dubessy, T. Badr, C. De Rossi, M. de Goër de Herve, L. Longchambon, and H. Perrin, Producing superfluid circulation states using phase imprinting, Phys. Rev. A **97**, 043615 (2018).
[52] Giacomo Roati, Phase imprinting on a ^{6}Li superfluid ring was demonstrated at LENS recently (private communication).
[53] E. Cameron, On the estimation of confidence intervals for binomial population proportions in astronomy: The simplicity and superiority of the Bayesian approach, Pub. Astron. Soc. Aust. **28**, 128 (2011).
[54] A. C. Mathey, C. W. Clark, and L. Mathey, Decay of a superfluid current of ultracold atoms in a toroidal trap, Phys. Rev. A **90**, 023604 (2014).
[55] A. Kumar, S. Eckel, F. Jendrzejewski, and G. K. Campbell, Temperature-induced decay of persistent currents in a superfluid ultracold gas, Phys. Rev. A **95**, 021602(R) (2017).
[56] M. Kunimi and I. Danshita, Decay mechanisms of superflow of Bose-Einstein condensates in ring traps, Phys. Rev. A **99**, 043613 (2019).
[57] M. A. Baranov and D. S. Petrov, Critical temperature and Ginzburg-Landau equation for a trapped Fermi gas, Phys. Rev. A **58**, R801 (1998).
[58] L. P. Gor'kov and T. K. Melik-Barkhudarov, Contribution to the theory of superfluidity in an imperfect fermi gas, Sov. Phys. JETP **13**, 1018 (1961).
[59] D. E. McCumber and B. I. Halperin, Time scale of intrinsic resistive fluctuations in thin superconducting wires, Phys. Rev. B **1**, 1054 (1970).
[60] D. R. Scherer, C. N. Weiler, T. W. Neely, and B. P. Anderson, Vortex Formation by Merging of Multiple Trapped Bose-Einstein Condensates, Phys. Rev. Lett. **98**, 110402 (2007).
[61] A. Das, J. Sabbatini, and W. H. Zurek, Winding up superfluid in a torus via Bose Einstein condensation, Sci. Rep. **2**, 352 (2012).
[62] G. B. Hess and W. M. Fairbank, Measurements of Angular Momentum in Superfluid Helium, Phys. Rev. Lett. **19**, 216 (1967).
[63] P. K. Chen, L. R. Liu, M. J. Tsai, N. C. Chiu, Y. Kawaguchi, S. K. Yip, M. S. Chang, and Y. J. Lin, Rotating Atomic Quantum Gases with Light-Induced Azimuthal Gauge Potentials and the Observation of the Hess-Fairbank Effect, Phys. Rev. Lett. **121**, 250401 (2018).
[64] B. Ko, J. W. Park, and Y. Shin, Kibble–Zurek universality in a strongly interacting Fermi superfluid, Nat. Phys. **15**, 1227 (2019); L. Corman, L. Chomaz, T. Bienaim, R. Desbuquois, C. Weitenberg, S. Nascimbne, J. Dalibard, and J. Beugnon, Phys. Rev. Lett. **113**, 135302 (2014).

[65] W. H. Zurek, Cosmological experiments in superfluid helium?, Nature (London) **317**, 505 (1985).

[66] T. Kashimura, S. Tsuchiya, and Y. Ohashi, Π-junction and spontaneous current state in a superfluid Fermi gas, Phys. Rev. A **84**, 013609 (2011).

[67] Y.-A. Liao, A. S. C. Rittner, T. Paprotta, W. Li, G. B. Partridge, R. G. Hulet, S. K. Baur, and E. J. Mueller, Spin-imbalance in a one-dimensional Fermi gas, Nature (London) **467**, 567 (2010).